Quantum Theory of Attosecond XUV Pulse Measurement by Laser Dressed Photoionization

Markus Kitzler, Nenad Milosevic, Armin Scrinzi, Ferenc Krausz, and Thomas Brabec*

Institut für Photonik, Technische Universität Wien, Gusshausstrasse 27/387, A-1040 Wien, Austria
(Received 31 August 2001; published 16 April 2002)

The first reported measurements of single attosecond pulses use laser dressed single-photon extreme ultraviolet (XUV) ionization of gas atoms. The determination of XUV pulse duration from the electron spectrum is based on a classical theory. Although classical models are known to give a qualitatively correct description of strong laser atom interaction, the validity must be scrutinized by a quantum-mechanical analysis. We establish a theoretical framework for the accurate temporal characterization of attosecond XUV pulses. Our analysis reveals an improved scheme that allows for direct experimental discrimination between single and multiple attosecond pulses.

Extreme ultraviolet (XUV) pulse durations are usually determined by a laser-XUV pulse cross-correlation measurement based on the laser-induced shift of the photoelectron spectrum [1–5]. The time resolution of this method is limited by the duration of the laser pulse and, therefore, cannot be used in the attosecond (10^{-18} sec, asec) time domain. Recently, several cross-correlation methods [6–9] were proposed that have the potential to resolve asec pulse durations. The most promising concept is based on the laser-induced shift of the photoelectron spectrum, that is produced by laser dressed single-photon ionization of gas atoms by an XUV asec pulse. Two modifications of this method were used to measure an asec pulse train [9] and an isolated XUV pulse with a duration of 650 asec [8]. Our investigation focuses on the scheme realized in Ref. [8], which has the advantage that single asec pulses can be measured. The difference to earlier experiments [1–5] is that the sublaser cycle resolution is achieved by measuring the electron spectrum only over a limited solid angle [8]. The XUV pulse duration was determined by using a classical model that relates the shift and the broadening of the electron spectrum to the XUV duration. The classical model allows efficient numerical implementation making this method a particularly attractive method for asec pulse measurement. Although classical models in strong laser-field physics are known to give a qualitatively correct description, quantitative agreement between a classical model and a full quantum-mechanical description is rarely the case. Therefore, a reliable determination of sub-fs pulse durations with laser dressed single XUV photoionization must depend on a thorough quantum-mechanical analysis.

We perform such an analysis using exact integration of the Schrödinger equation and analytical integration under the strong field approximation (SFA), where the influence of the atomic Coulomb potential on the free electrons is neglected. Based on the SFA we derive a quantum-mechanical and a semiclassical equation for the electron spectrum that can be integrated orders of magnitude faster than the Schrödinger equation. The semiclassical theory

presents a generalization of the classical model used in Ref. [8] and, in special cases, becomes identical with the classical model. The validity of the semiclassical approach is verified by a comparison to exact results, which in a certain parameter range yields good agreement. Finally, our analysis is used to identify an improved configuration for asec pulse measurement. This setup is more than 1 order of magnitude more efficient than the one used so far [8] and allows for direct experimental discrimination between single and multiple asec pulses.

Our analysis starts from the three-dimensional Schrödinger equation in atomic units,

$$i\partial_t \Psi(\mathbf{r}) = \left[-\frac{1}{2} \nabla^2 - \frac{1}{r} - \mathbf{r}E(t) \right] \Psi(\mathbf{r}), \quad (1)$$

where the electron is coupled to the classical electromagnetic field in dipole approximation and in the length gauge. Here, $\mathbf{r} = (x, y, z)$ denotes the space coordinates, ∇ is the corresponding gradient operator, ∂_t is the time derivative, and Ψ represents the electron wave function. The electric field $\mathbf{E}(t) = \mathbf{E}_l + \mathbf{E}_x$ comprises a laser, $\mathbf{E}_l$, and an XUV, $\mathbf{E}_x$, contribution. The laser and XUV components, $\mathbf{E}_{l,x} = \hat{\mathbf{e}}_{l,x} E_{l,x}(t - t_{l,x}) \cos[\omega_{l,x}(t - t_{l,x})]$, are characterized by the polarization vector $\hat{\mathbf{e}}_{l,x}$, envelope $E_{l,x}(t)$, and by the carrier frequency $\omega_{l,x}$. Further, we assume that the laser pulse peak is at $t_l = 0$ and that the XUV pulse peak is delayed by a time $t_x = t_d$. Finally, the electric field is related to the vector potential by $\mathbf{E} = -(1/c)\partial_t \mathbf{A}$, where c denotes the velocity of light.

In the following, Eq. (1) is solved analytically by applying the SFA [10], i.e., the Coulomb potential is neglected as compared to the laser field. As a result, the Coulomb continuum eigenfunctions may be substituted by plane waves, and Eq. (1) is integrated by using the ansatz $\Psi = |0\rangle \exp(iI_p t) + \int d^3 p\, b(\mathbf{p}, t) |\mathbf{p}\rangle$. Here, $|0\rangle$ denotes the ground state with ionization potential I_p, the plane wave is given by $|\mathbf{p}\rangle = \exp(i\mathbf{p}\mathbf{r})$ with $\mathbf{p}$ the electron momentum, and $b(\mathbf{p}, t)$ is the momentum space wave function of free electrons. Within the SFA we obtain the electron spectrum as [11]

$$b(\mathbf{p}) = i \int_{-\infty}^{\infty} \mathbf{E}(t')\mathbf{d}[\mathbf{p} - \mathbf{A}(t')]\exp\left[-i \int_{t'}^{\infty} \frac{1}{2}[\mathbf{p} - \mathbf{A}(t'')]^2 \, dt'' + iI_p t'\right] dt'. \tag{2}$$

The dipole moment is determined by $\mathbf{d}(\mathbf{p}) = \langle \mathbf{p}|\mathbf{r}|0\rangle$. For the special case of continuum transitions from hydrogen bound s states, $\mathbf{d} \propto \mathbf{p}/(\mathbf{p}^2 + 2I_p)^3$. For calculations in noble gases we have derived dipole moments from cross sections tabulated in Ref. [12].

The integral in Eq. (2) is calculated in two ways, by a Fourier-Bessel expansion of the exponential function in harmonics of the laser field [13] and by the stationary phase method [14]. The first route results in

$$|b(\mathbf{p})|^2 = \left| \sum_{n=-\infty}^{+\infty} i^n J_n(a, b) F_n(p) \right|^2, \tag{3}$$

where $F_n(p) = \int_{-\infty}^{+\infty} \mathbf{d} \cdot \mathbf{E}_x(t - t_d)\exp\{i[p^2/2 + I_p + U_p(t_d) + n\omega_l]t\} \, dt$, and $U_p(t) = E_l^2(t)/(4\omega_l^2)$ is the laser ponderomotive potential. The contributions F_n from the nth sideband are weighted by the generalized Bessel functions $J_n(a, b) = [\text{sgn}(-a)]^n \sum_{l=-\infty}^{+\infty} J_{n+2l}(|a|)J_{-l}(b)$ with $a = \mathbf{p} \cdot \hat{\mathbf{e}}_l E_l(t_d)/\omega_l^2$ and $b = E_l^2(t_d)/(8\omega_l^3)$. Note that Eqs. (3) and (2) give identical results as long as the XUV pulse duration is shorter than the laser optical cycle.

A simpler solution of Eq. (2) can be obtained in the semiclassical limit by stationary phase integration. This results in

$$|b(\mathbf{p})|^2 \approx \left| \sum_{t_s} \sqrt{\frac{\pi}{2i\ddot{S}(t_s)}} \mathbf{E}_x(t_s - t_d)\mathbf{d}[\mathbf{p} - \mathbf{A}(t_s)] \right.$$
$$\left. \times \exp[-iS(t_s)] \right|^2, \tag{4}$$

where $S(t_s) = (1/2) \int_{t_s}^{\infty} [\mathbf{p} - \mathbf{A}(t'')]^2 \, dt'' + (\omega_x - I_p)t_s$ is the classical action, and $\ddot{S}(t_s) = -E(t_s)[p\cos\theta - A(t_s)]$ is the second time derivative of the classical action. Here, θ denotes the angle between the momentum $\mathbf{p}$ and the polarization axis of the laser electric field. The stationary

phase points t_s are determined by solution of the stationary phase equation $(1/2)[\mathbf{p} - \mathbf{A}_l(t_s)]^2 = \omega_x - I_p$.

The SFA equation (3) and the semiclassical Eq. (4) reduce the computational effort for calculating the electron spectrum by 4 to 5 orders of magnitude as compared to the integration of Eq. (1). This makes the accurate determination of the XUV pulse duration including quantum effects practically possible. It will be shown below that Eq. (4) has a more limited validity range than Eq. (3); however, it has the advantage that contact can be made with the classical analysis of Ref. [8].

The asec pulse measurement method in Ref. [8] relies on the fact that the electron spectrum is measured in a limited solid angle θ, φ. The XUV pulse duration is determined by measuring the nth moment of the electron energy spectrum as a function of the XUV pulse delay t_d, which is given by

$$\langle \Omega^n(t_d) \rangle = \frac{\int_{\theta_0}^{\theta_1} \int_0^{\infty} \Omega^n |b(\Omega, \theta)|^2 \sqrt{\Omega} \, d\Omega \, \sin\theta d\theta}{\int_{\theta_0}^{\theta_1} \int_0^{\infty} |b(\Omega, \theta)|^2 \sqrt{\Omega} \, d\Omega \, \sin\theta d\theta}, \tag{5}$$

where we denote the electron energy by $\Omega = p^2/2$. The angle θ to the polarization axis is confined between θ_0 and θ_1. We focus here on configurations with cylindrical symmetry, where the linear laser and XUV polarizations coincide, for which the integral over φ drops out of Eq. (5). Usually, the center of gravity $\langle\Omega\rangle$ or the rms width of the electron spectrum $\Delta\Omega = \sqrt{\langle\Omega^2\rangle - \langle\Omega\rangle^2}$ is used for asec pulse measurement [8].

Equations (3) or (4) in combination with Eq. (5) allow an efficient numerical evaluation of $\langle\Omega^n\rangle$. With the use of Eq. (4), $\langle\Omega^n\rangle$ can be further simplified and yields a simple semiclassical formula. For that we insert Eq. (4) and transform from (Ω, θ) to (t_s, θ), where $\Omega(t_s)$ is defined by the stationary phase equation. This yields

$$\langle \Omega^n(t_d) \rangle = \frac{\int_{\theta_0}^{\theta_1} \int_{-\infty}^{\infty} \Omega^{n+1/2}(t_s)E_x^2(t_s - t_d)[\hat{\mathbf{e}}_x\mathbf{d}(t_s)]^2 \, dt_s \sin\theta d\theta}{\int_{\theta_0}^{\theta_1} \int_{-\infty}^{\infty} \Omega^{1/2}(t_s)E_x^2(t_s - t_d)[\hat{\mathbf{e}}_x\mathbf{d}(t_s)]^2 \, dt_s \sin\theta d\theta}. \tag{6}$$

Equation (6) puts the classical derivation of Ref. [8] on a more general and rigorous theoretical footing. In the special case of transitions to spherically symmetric s continuum waves (angular momentum $l = 0$), the result of Ref. [8] is exactly recovered. This is because, by virtue of the stationary phase condition, $\mathbf{d}$ becomes independent of the integration variables and drops out of Eq. (6).

The quality of the approximations utilized in our derivation was tested by comparison to an exact numerical solution of Eq. (1) based on a discretization of the Schrödinger equation in momentum space, as described in Ref. [15]. For Fig. 1 we calculated the rms width $\Delta\Omega$ in various ways. The modulation of $\Delta\Omega$ appears for pulses shorter than one laser half-cycle and gives a sensitive measurement of the XUV pulse duration. The modulation increases with decreasing XUV pulse

duration. The filled circles, solid line, and dotted line refer to the exact numerical solution of Eq. (1), to the SFA equation (3) in combination with Eq. (5), and to the integration of Eq. (6), respectively. The exact solution agrees well with the SFA solution, which demonstrates the validity of the SFA. The agreement with Eq. (6) is best around the laser pulse center. The reason is that the semiclassical calculation of the electron spectrum based upon the stationary phase method fails for vanishing laser intensities. In this limit, the electron spectrum becomes a delta peak at energy $\omega_x - I_p$. As a result $\Delta\Omega \to 0$ for large t_d, whereas in reality the width never drops below the spectral width of the XUV pulse. The calculations in Fig. 1 were repeated by varying the laser and XUV pulse parameters in the range relevant for asec pulse measurement (XUV/laser duration between
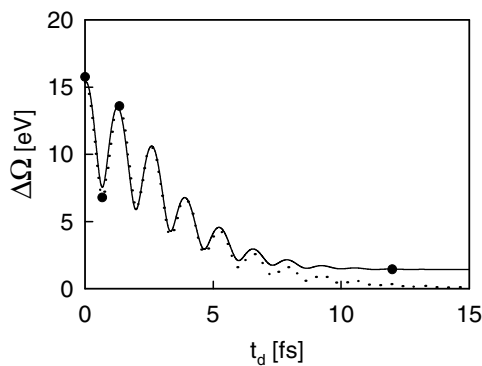
FIG. 1.   rms width $\Delta\Omega$ of the electron spectrum for a hydrogen ($1s$) ground state as a function of delay time, t_d, between the laser and XUV pulse. The pulse parameters are laser wavelength $\lambda_l = 800$ nm, laser FWHM pulse duration 5 fs, sech laser pulse envelope, laser intensity $I_l = 3 \times 10^{13}$ W/cm^2, $\omega_x = 90$ eV, XUV pulse duration 500 asec, XUV pulse intensity $I_x = 10^{12}$ W/cm^2. Laser and XUV polarization are chosen parallel to the direction of observation, $\hat{\mathbf{z}} = \hat{\mathbf{e}}_l \parallel \hat{\mathbf{e}}_x \parallel \mathbf{p}$, and $\theta_1 = 2°$. $\Delta\Omega$ was calculated in various ways: exact numerical solution of Eq. (1) (filled circles), evaluation of the SFA equation (3) (solid line), and integration of the semiclassical Eq. (6) (dotted line).

0.1/5 and 1/15 fs, XUV/laser peak intensity between 10^{12} and 10^{14} W/cm^2, sech, and Gaussian pulse shape). The only parameter critical for the applicability of the semiclassical model is the laser peak intensity, for the reasons discussed above. For intensities well below 10^{13} W/cm^2 the semiclassical theory predicts wrong rms widths (see Fig. 1) and the SFA equation must be used. Finally, we did not plot the classical result, which is identical with the semiclassical calculation for the parameters chosen here. This is because for $\theta \approx 0°$, $\mathbf{d}$ becomes again independent of the integration variables and drops out of Eq. (6). For $\theta \approx 90°$ the effect of $\mathbf{d}$ is maximum and introduces a factor of 2 in the modulation depth of the rms width.

To further corroborate the applicability of the SFA, we have compared electron spectra in Fig. 2, which were calculated by an exact solution of Eq. (1) (solid line) and by Eq. (3) (dotted line). The agreement is excellent, justifying the omission of the Coulomb potential in the derivation of Eq. (3). Figure 2 reveals another important result. Except for the XUV photoelectrons the spectrum at low energies contains a contribution of ATI (above-threshold ionization) electrons generated by the laser directly. The experimental setup must be chosen in such a way that the two contributions fall into well-separated spectral ranges. Otherwise the laser dressed photoionization signal, carrying the information on the asec pulse duration, is covered by the ATI electrons. So far, in order to minimize ATI, electrons were observed perpendicular to the laser polarization axis [8]. The spectrum in Fig. 2 shows that the level of ATI electrons is less than anticipated. Even for $\hat{\mathbf{e}}_l \parallel \mathbf{p}$, where ATI reaches the maximal energies, the laser induced part of the ionization spectrum is well separated from the x-ray photo ionization spectrum.
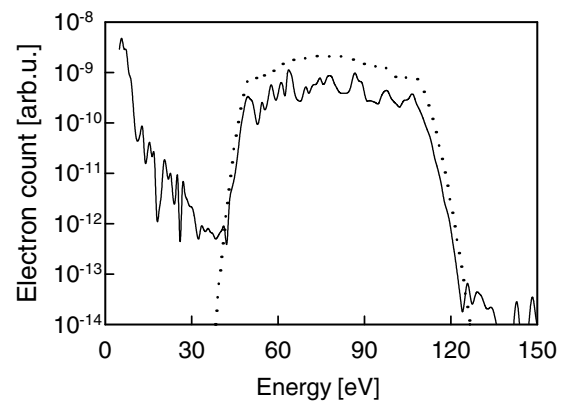

FIG. 2.   Photoelectron spectrum for the parameters of Fig. 1 and delay $t_d = 0$. The solid and dotted lines denote the electron spectrum as determined by numerical integration of the Schrödinger equation (1) and the SFA equation (3), respectively. Note that, in the derivation of Eq. (3), laser-induced ionization is not included, which is responsible for the low-frequency part (<30 eV) in the exact calculation.

This can be understood from a simple estimate. The laser-induced part of the ATI spectrum consists of a main part extending to $2U_p$ and a smaller contribution coming from rescattering, with electron energies up to $10U_p$ [16]. Only the $2U_p$ contribution is strong enough to cover the XUV-induced electron signal. As a result, asec-pulse measurement is feasible, as long as the lower cutoff of the XUV photoelectron spectrum does not overlap with the $2U_p$ part of the laser-induced ATI spectrum. Based on the stationary phase equation derived above the simple condition $8U_p \leq \omega_x - I_p$ is found, determining the parameter range in which the two spectral contributions remain seperate. Laser-induced ionization becomes dominant and buries the single XUV photoionization signal only for laser peak intensities in excess of 10^{14} W/cm^2. This finding adds an additional degree of freedom to the realization of an optimum setup for asec pulse measurement.

A major problem in asec-pulse measurements is the low efficiency of harmonic sources and the resulting long data collection times and poor signal-to-noise ratio. So far the asec measurement was performed with Kr $4p$ electrons, for which the single XUV photon ionization is dominated by a transition to a spherically symmetric s continuum wave [12]. We have compared various experimental setups with respect to efficiency in electron yield. We find an optimal setup when laser and x-ray polarization are chosen parallel to the direction of observation of the electron spectrum, i.e., $\hat{\mathbf{e}}_l \parallel \hat{\mathbf{e}}_x \parallel \mathbf{p}$. Instead of Kr $4p$ we propose to use Ne $2p$ electrons. The overall gain in the XUV electron yield as compared to the setup in Ref. [8] is a factor of 30 for the same opening angle of 40°. This enhancement can be attributed to two reasons. First, the Ne $2p$ transition is an order of magnitude more efficient than the Kr $4p$ transition. Second, the XUV photoionization (90 eV) of Ne $2p$ electrons is dominated by a transfer into a d continuum wave, which extends in the direction
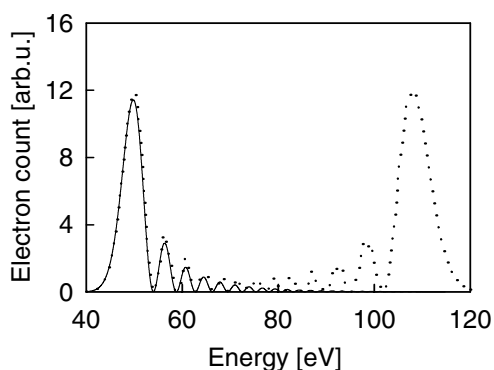
FIG. 3. Signature of two attosecond pulses with delay times $t_d = \pm 1/4$ laser optical cycles compared to a single pulse with delay $t_d = 1/4$. The remaining pulse parameters are as in Fig. 1. Electrons released at $t_d = \pm 1/4$ experience maximal acceleration and maximum deceleration by the laser, creating two well-separated electron peaks (dotted line). A single pulse creates only a single peak (solid line).

of the x-ray polarization. Therefore, a measurement along the x-ray polarization direction captures a larger part of the photoelectrons, which gives an enhancement by a factor of 3. The gain enhancement by more than 1 order of magnitude in our improved setup makes a more efficient measurement of asec pulses possible and allows an extension of the method towards shorter wavelengths.

Higher harmonic generation with few cycle laser pulses tends to generate a single asec pulse with satellites at a repetition rate of twice the laser frequency. For practical applications it is essential to discriminate between a single asec pulse and a pulse train. Recently, indirect evidence of single asec pulses was obtained by using the harmonic spectrum [8]. Measurement of the electron spectrum in the laser polarization direction will allow for the first time to directly distinguish a single asec pulse from a pulse train (see Fig. 3). This is because the shift of electron energies becomes sensitive to the sign of the laser vector potential at the time of XUV ionization. Depending on the sign, electrons are either accelerated or decelerated by the laser, leading to two well-separated peaks in the electron spectrum. For one main and one or two smaller satellite pulses, the ratio of the peaks in the electron spectrum reflects the relative energy content carried in the satellites. In an experiment, data are usually collected over several shots. For the observation of a single peak, it is essential that the absolute phase of the laser field is kept constant during data acquisition.

In conclusion, we have developed a quantum-mechanical model of laser dressed single x-ray photoionization. It was shown that laser dressed photoionization can be quantitatively modeled by using the strong field approximation, i.e., by neglecting the Coulomb potential during the continuum evolution of the electron. Based on the strong field approximation, we derived a quantum-mechanical and a semiclassical expression that can be evaluated efficiently, making an accurate determination of the asec pulse duration including quantum effects practicable. The validity range of the previously used classical model was established. We identified an optimum setup for an asec pulse measurement that is a factor of 30 more efficient than existing schemes. Finally, the proposed setup discriminates between single and multiple attosecond pulses. The results revealed by our quantum-mechanical investigation open the way towards an accurate and more efficient measurement of asec pulses.

*Email address: brabec@tuwien.ac.at
[1] J. M. Schins et al., Phys. Rev. Lett. **73**, 2180 (1994).
[2] J. M. Schins et al., J. Opt. Soc. Am. B **13**, 197 (1996).
[3] T. E. Glover, R. W. Schoenlein, A. H. Chin, and C. V. Shank, Phys. Rev. Lett. **76**, 2468 (1996).
[4] A. Bouhal et al., J. Opt. Soc. Am. B **14**, 950 (1997).
[5] E. S. Toma et al., Phys. Rev. A **62**, 061801(R) (2000).
[6] E. Constant, V. D. Taranukhin, A. Stolow, and P. B. Corkum, Phys. Rev. A **56**, 3870 (1997).
[7] A. Scrinzi, M. Geissler, and T. Brabec, Phys. Rev. Lett. **86**, 412 (2001).
[8] M. Drescher et al., Science **291**, 1923 (2001); M. Hentschel et al., Nature (London) **414**, 509 (2001).
[9] P. M. Paul et al., Science **292**, 1689 (2001).
[10] L. V. Keldysh, Sov. Phys. JETP **20**, 1307 (1965).
[11] T. Brabec and F. Krausz, Rev. Mod. Phys. **72**, 545 (2000).
[12] U. Becker and D. A. Shirley, *VUV and Soft X-ray Photoionization* (Plenum, New York, 1996).
[13] M. Abramowitz and I. A. Stegun, *Handbook of Mathematical Functions* (Dover, New York, 1972).
[14] C. M. Bender and S. A. Orszag, *Advanced Mathematical Methods for Scientists and Engineers* (McGraw Hill, New York, 1978).
[15] A. Scrinzi, T. Brabec, and M. Walser, in *Proceedings of the Workshop on Super-Intense Laser-Atom Physics,* edited by B. Piraux and K. Rzaszewski (Kluwer, Dordrecht, 2001), p. 313.
[16] D. B. Milosevic and F. Ehlotzky, Phys. Rev. A **58**, 3124 (1998).